Geometry engineering for the RF behavior of low-dimensional gate-all-around transistors

A. Benali, F. L. Traversa, G. Albareda, M. Aghoutane *, and X.Oriols
Electronic Engineering Department Universitat Autònoma de Barcelona Bellaterra, Barcelona 08193
*Universidad Abdelmalek Essaâdi, 93000, Tetuán, Morocco
Email: abdelilah.benali@uab.es

***Abstract*—The aim of this work is to show the dependence of the time dependent current of gate-all-around transistors on their geometries and thus to find out how to optimize their intrinsic AC behavior. The Ramo-Shockley-Pellegrini (RShP) theorem and many-particle Monte Carlo technique are used, through the recently developed BITLLES simulator which is devoted to simulate classical and quantum electronic devices, to tackle this problem. Analytical and Monte Carlo (MC) simulations show how the HF spectrum noticeably depends on the ratio between lateral (Ly,Lz) and longitudinal (Lx) dimensions of a gate-all-around transistor.**

I. Introduction

The RF characterization of nanostructure is a relevant issue for the modern and future electronic devices. However, theoretical predictions of their frequency dependent behavior is a very challenging task. Indeed, being nanoelectronic rapidly approaching Terahertz operating regimes, at such frequencies the electric current is not only controlled by the flux of electrons crossing a particular surface (conduction current), but also by the temporal variations of the electric field (displacement current).

Since the electric field inside the active region device is strongly influenced by the device geometry, one can expect that these elements can have a strong influence on the displacement current and, in turn, on the RF behavior of the next-generation of nanoscale transistors.
This work is organized starting with an analytical computation of power spectral density (PSD) to qualitatively point out how the the geometry can affect it. Then we report numerical calculation of PSD sought for by Monte Carlo simulation and finally the last section id devoted to discuss the role played by transistor geometries in determining AC behavior of electronic devices.

II. High-frequency noise dependence on the device geometry

The direct computation of the time-dependent total (conduction and displacement) current accounts of numerical difficulties when implemented exploiting spatial grids and finite time-steps [1]. Alternatively, RShP theorem [2], [3], [4] is free from those limitations and provides an accurate relationship between the total current and electron dynamics. Furthermore RShP theorem also provides a simple and analytical way to describe the total current in simple geometries. For both these reasons we will employ RShP formalism in our treatment.

A. Analytical results

We consider an electronic device whose active region is delimited by the volume $\Omega = L_x \times L_y \times L_z$ which is depicted in Fig. 1 . The schematic representation showed in Fig. 1 is designed using BITLLES simulator. Let us consider N electrons traversing the volume Ω with constant velocity $\vec{v} = (v_x, 0, 0)^T$ in the transport direction x, from source to drain .Then, the total time dependent current at the ith surface can be calculated using RShP theorem and it reads

$$\begin{aligned} I_i(t) &= \Gamma_i^q(t) + \Gamma_i^e(t), \\ \Gamma_i^q(t) &= -\sum_{j=1}^{N} \vec{F}_i(\vec{r}_j[t]) \cdot |q| \cdot \vec{v}_j(\vec{r}_j[t]), \\ \Gamma_i^e(t) &= \int_S \epsilon(\vec{r}) \cdot \vec{F}_i(\vec{r}) \cdot \frac{\partial V(\vec{r},t)}{\partial t} \cdot d\vec{s}, \end{aligned} \tag{1}$$

where $\vec{r}_j[t]$ is the position of the jth electron at time t, the function $V(\vec{r}, t)$ is the scalar potential at position $\vec{r}$ and time t, $\epsilon(\vec{r})$ is the non-uniform electric permittivity depending on space and q is elementary electron charge.

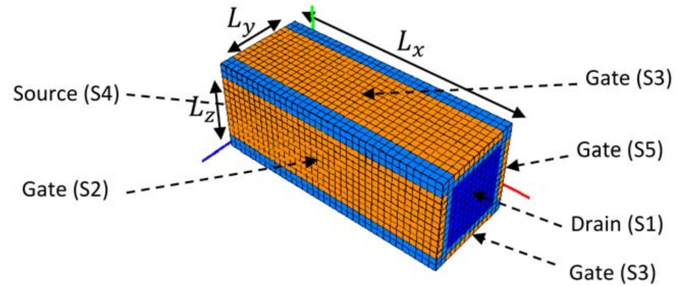

Fig. 1. *Schematic representation of a gate-all-around transistor. The channel dimensions are L_x, L_y and L_z and it is limited by the closed surface $S = \{S_1, ..., S_6\}$. Transport takes place from source to drain.*

We define a set of scalar functions (one set for each particular surface S_i) $\Phi_i(\vec{r})$ and its associated vector functions $\vec{F}_i(\vec{r})$, through:

$$\vec{F}_i(\vec{r}) = -\vec{\nabla}\Phi_i(\vec{r}). \tag{2}$$

These functions $\Phi_i(\vec{r})$ and $\vec{F}_i(\vec{r})$ fulfill the equations:

$$\vec{\nabla}(\epsilon(\vec{r}) \cdot \vec{F}_i(\vec{r})) = -\vec{\nabla}(\epsilon(\vec{r}) \cdot \vec{\nabla}\Phi_i(\vec{r})) = 0, \tag{3}$$

and the following particular Dirichlet boundary condition on the definition of $\Phi_i(\vec{r})$ are considered:

$$\Phi_i(\vec{r}) = 1; \vec{r} \in S_i \text{ and } \Phi_i(\vec{r}) = 0; \vec{r} \in S_{h\neq i} \quad (4)$$

meaning that $\Phi_i(\vec{r}) = 1$ on the surface S_i and zero on the other surfaces.

The subindex i means that we have six different possible sets of functions, one for each surface S_i. All functions $\Phi_i(\vec{r})$ and $\vec{F}_i(\vec{r})$ share the same defining equations (2) and (3), but different boundary conditions (4).

In order to analyze the dependence of the total time dependent current and spectrum noise on the geometries, in particular on the ratio between lateral (Ly,Lz) and longitudinal (Lx) dimensions, we need to solve Laplace's equation (3). However, the boundary conditions which would be used, for instance, to compute the current on the surface S_1 are $\Phi_1(\vec{r}) = 1; \vec{r} \in S_1$ and $\Phi_i(\vec{r}) = 0; \vec{r} \in S_{i\neq 1}$.

We assume the particular volume Ω depicted in Fig. 1 with an uniform dielectric constant. Under such simple geometry, the solution for the scalar function $\phi_1(\vec{r})$ can be written as [5]:

$$\phi_1(\vec{r}) = \frac{16}{\pi^2} \sum_{i=1,3,5..}^{\infty} \sum_{j=1,3,5..}^{\infty} \left[\frac{\sinh\left(\pi\sqrt{(\frac{i}{L_y})^2 + (\frac{j}{L_z})^2} \cdot x\right)}{i \cdot j \cdot \sinh\left(\pi\sqrt{(\frac{i}{L_y})^2 + (\frac{j}{L_z})^2} \cdot L_x\right)}\right] \cdot [\sin(\frac{i\pi}{L_y} y) \cdot \sin(\frac{j\pi}{L_z} z)]. \quad (5)$$

Let us discuss the approximation of $\phi_1(\vec{r})$ for two limit cases: $Lx << Ly, Lz$ and $Lx >> Ly, Lz$. The former limit leads to the approximations [6]

$$\phi_1(\vec{r}) \approx \frac{x}{L_x}, \quad (6)$$

$$\vec{F}_1(\vec{r}) \cdot \vec{x} = -\vec{\nabla}\Phi_i(\vec{r}) \cdot \vec{x} \approx -\frac{1}{L_x}. \quad (7)$$

Neglecting the second term in (1) [6] and using (7), we found,

$$\Gamma_1^q(t) = I_1(t) \approx \frac{|q| v_x}{L_x}, \quad (8)$$

Now consider the latter limit case $Lx >> Ly, Lz$. The functions $\phi_1(\vec{r})$ and $\vec{F}_1(\vec{r})$ can be approximated by [6]

$$\phi_1(\vec{r}) \approx \; exp\left(\pi\sqrt{(\frac{1}{L_y})^2 + (\frac{1}{L_z})^2} \cdot (x - L_x)\right), \quad (9)$$

$$\vec{F}_1(\vec{r}) \cdot \vec{x} = -\vec{\nabla}\Phi_i(\vec{r}) \cdot \vec{x} \approx -\alpha_x \cdot exp\left(\alpha_x(x - L_x)\right). \quad (10)$$

and the corresponding current in this case reads,

$$\Gamma_1^q(t) = I_1(t) \approx |q|\alpha \cdot e^{\alpha(t-\tau)}, \quad (11)$$

where τ is the electron transit time that is defined as $\tau = L_x/v_x$, $\alpha = v_x \alpha_x$ and $\alpha_x = \pi\sqrt{(\frac{1}{L_y})^2 + (\frac{1}{L_z})^2}$.

We now analytically compute the AC spectrum for the two different extreme device geometries. On the one hand, the PSD corresponding to the current expression (8) is given by:

$$PSD_1(\omega) = 2q^2\nu \frac{sin^2(\omega\tau/2)}{(\omega\tau/2)^2}, \quad (12)$$

on the other hand , for expression (11) we find,

$$PSD_1'(\omega) = 2q^2\nu' \frac{1}{1 + (\omega/\alpha)^2}, \quad (13)$$

where ν and ν' are the injection rates corresponding respectively to $L_y, L_z \gg Lx$ and $L_y, L_z \ll Lx$. In Fig. 2 $PSD_1(\omega)$ (blue squares line) and, $PSD_1'(\omega)$ (black circles line) are reported. We clearly see that decreasing the lateral section area

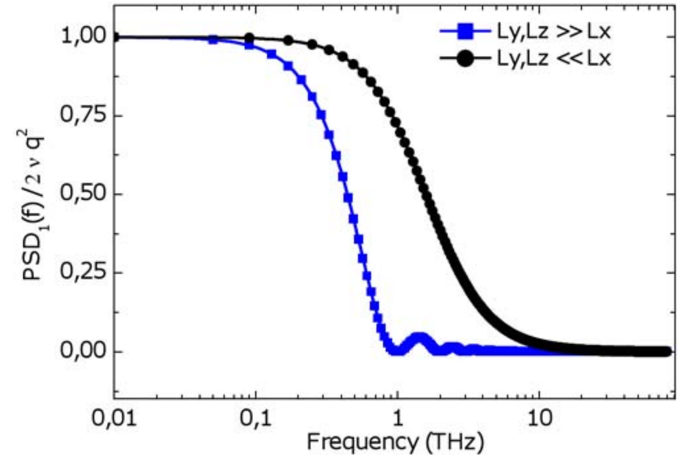

Fig. 2. *$PSD(f)$ (in units of $2q^2\nu$ where ν is the injection rate) for the analytical current equation (8) (blue squares) and (11) (black spots) for non-correlated transmitted electrons moving with constant velocity $v_x = 10^5 m/s$.*

(L_y, L_z) keeping longitudinal dimension (L_x), the spectrum noise frequency range moves to high frequency. This is the result that we would like to find out by means of Monte Carlo simulations in the next paragraph.

B. Monte Carlo results

In order to confirm previous results, we have carried out simulations of the total current implementing the RShP theorem mentioned above into a many-particle Monte Carlo simulator named BITLLES [7] employing either classical or Bohmian (quantum) trajectories [7], [8]. The BITLLES simulator have been recently developed by X. Oriols and his coworkers. This simulator is able to calculate the time-dependent current in electronic devices by including the self-consistent solution of electron transport and Poisson equations, beyond the standard mean-field approximation [9]. In particular, the noise spectrum of a gate-all-around Silicon nanowire (which is a typical multigate structure avoiding short-channel effects with a low-dimensional channel to reach higher mobilities) has been simulated.

In this simulation, we consider a gate-all-around Silicon

nanowire depicted in Fig. 1. We assume the transport along the (100) channel orientation (we use an electron effective mass equal to 0.19 times the electron free mass). An uniform relative permittivity equal to 11.75 in the whole volume Ω is considered. We consider two particular device geometries.

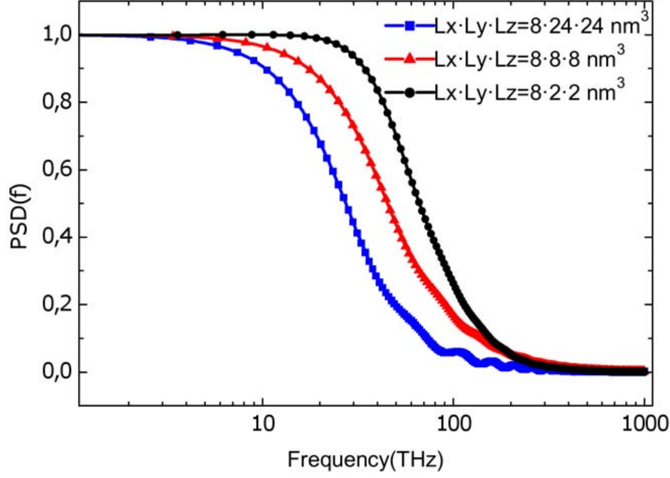

Fig. 3. *Normalized $PSD(f)$ of non-correlated transmitted electrons. Three different geometries, with same longitudinal dimension (Lx) and different section area (L_y, L_z), are compared using Monte Carlo simulation for gate-all-around Silicon nanowire.*

In Fig. 3, the numerical PSDs for three different geometries $(Lx \cdot Ly \cdot Lz = 8 \cdot 24 \cdot 24nm^3)$, $(Lx \cdot Ly \cdot Lz = 8 \cdot 8 \cdot 8nm^3)$ and $(Lx \cdot Ly \cdot Lz = 8 \cdot 2 \cdot 2nm^3)$ are reported confirming the simpler analytical results.

C. Understanding the results

Before commenting our results, we would like to highlight a possible source of confusion about the application of the RShP theorem appears when the current on a surface of the volume Ω (for example $I_4(t)$) is directly interpreted as the current measured in the ammeter. This is not always the case as can be seen in Fig. 4.

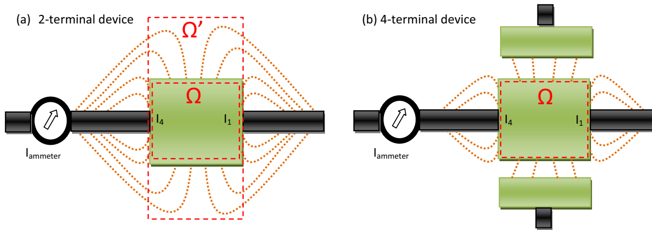

Fig. 4. (Color online) (a) A 2-terminal device where the $I_4(t)$ is not equal to $I_{ammeter}(t)$ because the lines of the electric field on the other surfaces of the volume Ω end close to the ammeter without crossing the surface S_4. (b) A 4-terminal device where $I_4(t) = I_{ammeter}(t)$.

For the 2-terminal device and the volume Ω plotted in Fig. 4(a), the current $I_4(t)$ is clearly different from the current in the ammeter $I_{ammeter}(t)$. The time-dependent variations of the electric field on the surfaces different from S_4 reach the ammeter without crossing S_4. The current on the ammeter is then equal to $I'_4(t)$ where the "acute accent"means that we have used the volume Ω' in Fig. 4(a). Since the explicit simulation of Ω' to obtain $I_{ammeter}(t)$ is not trivial because it demands a very large simulation box, alternatively, one can use the smaller volume Ω by modifying the Dirichlet boundary conditions used in (2). Fortunately, for state-of-the art gate-all-around transistors used to avoid short-channel effects, the assumption that $I_4(t)$ is the total current at the ammeter, $I_{ammeter}(t)$, becomes fully accurate. See Fig. 4 (b). This work will only consider such gate-all-around transistors with a fixed voltage on all the surfaces(S_1 drain, S_4 source and $\{S_2, S_3, S_5, S_6\}$ gates).

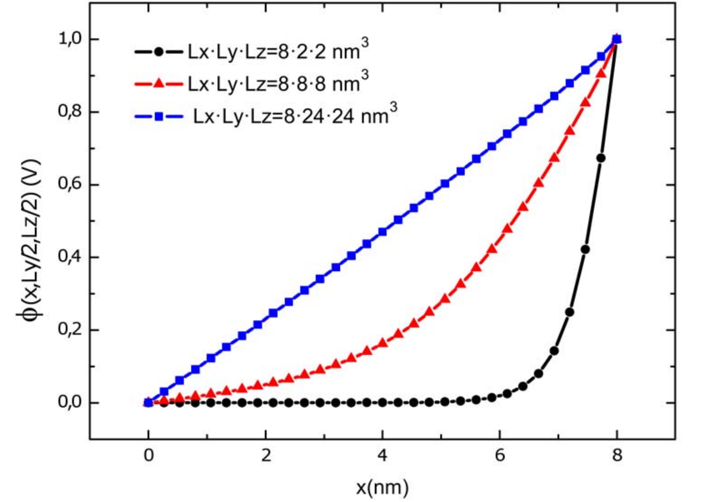

Fig. 5. *Representation of $\phi_1(\vec{r})$ (a.u.) along the points for three particular geometries. In each geometry, the roles of y and z are interchangeable. The geometries considered here are $(Lx \cdot Ly \cdot Lz = 8 \cdot 24 \cdot 24nm^3)$, $(Lx \cdot Ly \cdot Lz = 8 \cdot 8 \cdot 8nm^3)$ and $(Lx \cdot Ly \cdot Lz = 8 \cdot 2 \cdot 2nm^3)$ and are respectively showed by blue solid square, red solid triangle and black solid circle (when they are presented in color).*

With aim of explaining how the spectrum noise vary in the analytical and numerical case, we have illustrated in Fig. 5 the function $\phi_1(\vec{r})$ solution of Laplace's equation (3) for three different gate-all-around transistor geometries.

The geometries chosen for this purpose are $(Lx \cdot Ly \cdot Lz = 8 \cdot 24 \cdot 24nm^3)$, $(Lx \cdot Ly \cdot Lz = 8 \cdot 8 \cdot 8nm^3)$ and $(Lx \cdot Ly \cdot Lz = 8 \cdot 2 \cdot 2nm^3)$ and are respectively showed in Fig. 5 by blue solid square, red solid triangle and black solid circle.

We observe in Fig. 5 that fixing $Lx = 8nm$ and dropping down the total lateral area from $(Ly \cdot Lz) = (24 \cdot 24)nm^2$ to $(Ly \cdot Lz) = (2 \cdot 2)nm^2$, the function $\phi_1(\vec{r})$ changes from a linear shape to an approximately exponential one. The latter shapes correspond to the limit cases reported in the equations (6) and (9). On the other hand, the variation of ϕ_1 directly affects its associated vector function $\vec{F}_1$ reported in Fig. 6. Notice that $\vec{F}_1$ is the direct responsible for the variations of the time dependent current through the equations (1)(second expression).

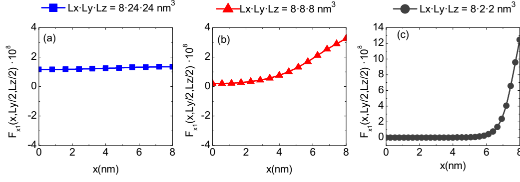

Fig. 6. *(a), (b) and (c), numerical computation of the function $\vec{F}_1(\vec{r})$ in the transport direction, respectively, for geometries $(Lx{\cdot}Ly{\cdot}Lz = 8{\cdot}24{\cdot}24nm^3)$, $(Lx \cdot Ly \cdot Lz = 8 \cdot 8 \cdot 8nm^3)$ and $(Lx \cdot Ly \cdot Lz = 8 \cdot 2 \cdot 2nm^3)$.*

For a deeper comprehension of the effect of $\vec{F}_1$ of the PSD, we analyze the motion of an electron crossing the gate-all-around transistor in x-direction (from source to drain). This is carried out through BITLLES simulator. The geometries considered are the same previously mentioned. Numerical self-consistent contribution of one trajectory in a gate-all-around transistor structure to the term $\Gamma_1^q(t)$ is showed in Fig.7.

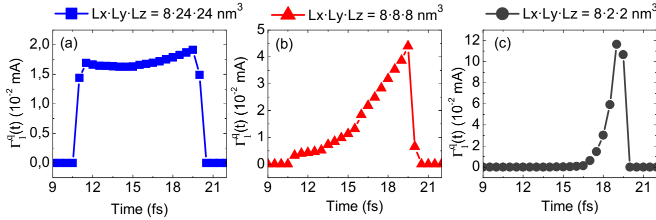

Fig. 7. *(a), (b) and (c), numerical self-consistent contribution of one trajectory in a gate-all-around transistor structure to the term $\Gamma_1^q(t)$ when three different volumes Ω presented at 6 are considered*

We deduce, comparing figures 6 and 7 that the time dependent current due to a single electron, noticeably follows the $\vec{F}_1(\vec{r})$ shapes in spite of the fact that the current is also explicitly dependent on the electron velocity. The function $\vec{F}_1$ depends only on the space $\vec{r}$, this means that the time dependent current crossing a device is strongly affected by its geometry, in other words looking at Fig. 7, decreasing the lateral area the time dependent current narrows down. Contextually the autocorrelation abruptly changes when the signal associated to the one-electron current gets narrow. This is the reason why the spectrum noise moves to very high frequency.

III. Conclusion

We have demonstrated that the AC current of gate all around transistor drastically depends on the device geometry. We have found out, by analytical and MC simulations, that PSD shapes are determined by the ratio between the lateral and longitudinal dimensions. This work opens a new path to engineers to optimize nanoelectronic device geometries in order to improve their THz AC performance.

Acknowledgment

This work has been partially supported through MEC project MICINN TEC2009-06986 and by the ”Agencia Espaola de Cooperacin internacinal para el Desarrollo” (AECID).

References

[1] A. Alarcón and X. Oriols, *Journal of Statistical Mechanics: Theory and Experiment*. 2009, P01051 ,2009.
[2] S. Ramo, *Proceedings of the I. R. E.* , 27, 584 ,1939.
[3] W. Shockley, *J. Appl. Phys.* 9, 635 ,1938.
[4] B. Pellegrini, *Physical Review B*, 34(8), 5921 ,1986.
[5] J. D. Jackson *Classical Electrodynamics, 3rd Ed. John Wiley and Sons* , 1975.
[6] A. Benali et al. , *Fluctuation and Noise Letters*, submited.
[7] http://europe.uab.es/bitlles
[8] X. Oriols, *Phys. Rev. Lett.* 98 066803, 2007.
[9] G. Albareda, J. Suñé and X. Oriols, *Phys. Rev.* B, 79(7) 075315, 2009.